



ELSEVIER

Contents lists available at ScienceDirect

Journal of Solid State Chemistry

journal homepage: www.elsevier.com/locate/jssc

Pyrochlore “dynamic spin-ice” $\text{Pr}_2\text{Sn}_2\text{O}_7$ and monoclinic $\text{Pr}_2\text{Ti}_2\text{O}_7$: A comparative temperature-dependent Raman study

Surajit Saha^a, Sudakshina Prusty^{a,1}, Surjeet Singh^{b,2}, R. Suryanarayanan^b,
A. Revcolevschi^b, A.K. Sood^{a,*}

^a Department of Physics, Indian Institute of Science, Bangalore 560012, India

^b Laboratoire de Physico-Chimie de l'Etat Solide, ICMMO, CNRS, UMR8182, Universite Paris-Sud, 91405 Orsay, France

ARTICLE INFO

Article history:

Received 12 February 2011

Received in revised form

20 June 2011

Accepted 21 June 2011

Available online 29 June 2011

Keywords:

Pyrochlore

Raman spectroscopy

Phonon anharmonicity

Crystal-field splitting

ABSTRACT

Here we report a temperature-dependent Raman study of the pyrochlore “dynamic spin-ice” compound $\text{Pr}_2\text{Sn}_2\text{O}_7$ and compare the results with its non-pyrochlore (monoclinic) counterpart $\text{Pr}_2\text{Ti}_2\text{O}_7$. In addition to phonon modes, we observe two bands associated with electronic Raman scattering involving crystal field transitions in $\text{Pr}_2\text{Sn}_2\text{O}_7$ at ~ 135 and 460 cm^{-1} which couple strongly to phonons. Anomalous temperature dependence of phonon frequencies that are observed in pyrochlore $\text{Pr}_2\text{Sn}_2\text{O}_7$ are absent in monoclinic $\text{Pr}_2\text{Ti}_2\text{O}_7$. This, therefore, confirms that the strong phonon–phonon anharmonic interactions, responsible for the temperature-dependent anomalous behavior of phonons, arise due to the inherent vacant sites in the pyrochlore structure.

© 2011 Elsevier Inc. All rights reserved.

1. Introduction

Spins in the geometrically frustrated pyrochlores ($A_2B_2O_7$, $A =$ rare-earth ion, $B = \text{Ti, Zr, Ir, Sn, ...}$) are known to show complex magnetic ground states ranging from spin-liquid and spin-glass to spin-ice behavior [1–3]. In these systems, an interplay among the crystal electric field, magnetic exchange and the dipolar interactions results in realizing an appropriate ground state. In general, the exchange interaction in these systems are antiferromagnetic in nature and are much stronger than the crystal field and dipolar interactions. A delicate balance among these three interactions leads to, for example, the spin-liquid state in $\text{Tb}_2\text{Ti}_2\text{O}_7$ [4–6]. When the dipolar interactions dominate over the exchange interactions with an Ising-like anisotropy along the $\langle 111 \rangle$ direction, spin-ice ground state is realized in pyrochlores $\text{Ho}_2\text{Ti}_2\text{O}_7$ and $\text{Dy}_2\text{Ti}_2\text{O}_7$ [7–9]. Spin-ice is a very special case of the various magnetic ground states realized in geometrically frustrated pyrochlores. Here the spins at the corners of each tetrahedron freeze into a two-in-two-out configuration, analogous to the two-short-two-long proton bond disorder in “water-ice”—both the states having an exactly

same zero-point entropy $\frac{1}{2}R \ln\left(\frac{3}{2}\right)$ [8,10–12]. Realization of this exotic ground state (spin-ice) in pyrochlores was known to be limited to the compounds of the rare-earth elements with large magnetic moments ($\mu \sim 10\mu_B$) and strong nearest neighbor dipolar interactions, such as $\text{Ho}_2\text{Ti}_2\text{O}_7$ [7], $\text{Dy}_2\text{Ti}_2\text{O}_7$ [11], $\text{Ho}_2\text{Sn}_2\text{O}_7$ [13], $\text{Dy}_2\text{Sn}_2\text{O}_7$ [14]. However, recently, a “dynamic spin-ice” state has been seen in $\text{Pr}_2\text{Sn}_2\text{O}_7$ at low temperatures where the dipolar interaction ($D_{NN} = (5/3)(\mu_0/4\pi)(\mu^2/r_{NN}^3) = 0.13\text{ K}$, where $r_{NN} =$ nearest neighbor A^{3+} distance) is almost 20 times smaller than that of the conventional dipolar spin-ice compounds mentioned above (where $D_{NN} \sim 2.5\text{ K}$) and is also much weaker than its magnetic exchange energy ($J_{NN}/D_{NN} = 7.1$) [15]. Zhou et al. showed that the zero-point entropy of $\text{Pr}_2\text{Sn}_2\text{O}_7$ is $\sim 25\%$ higher than that of the Ho/Dy-based spin-ice, thus indicating that the spins in $\text{Pr}_2\text{Sn}_2\text{O}_7$ spin-ice are more dynamic than in the conventional dipolar spin-ice (and hence the name “dynamic spin-ice”) and proposed that the spin dynamics, which is due to crystal field anisotropy, is carried over by a tunneling process between the various equivalent two-in-two-out configurations [15].

The vibrational properties of the pyrochlores have also been investigated in recent years revealing anomalous temperature dependence and phase transitions [16–27]. It was seen that phonon frequencies in several pyrochlore titanates, e.g., $\text{Er}_2\text{Ti}_2\text{O}_7$ [18], $\text{Gd}_2\text{Ti}_2\text{O}_7$ [18,19], $\text{Dy}_2\text{Ti}_2\text{O}_7$ [16,18–20], decrease on lowering the temperature. Since this anomalous behavior was also seen for the phonons in non-magnetic pyrochlore $\text{Lu}_2\text{Ti}_2\text{O}_7$ [16], the possible origin was attributed to strong phonon–phonon anharmonic interactions and not to spin–phonon coupling [16].

* Corresponding author.

E-mail addresses: asood@physics.iisc.ernet.in,

saha.surajit@gmail.com (A.K. Sood).

¹ Presently at National Institute of Science Education and Research, Bhubaneswar 751005, India.

² Presently at Indian Institute of Science Education and Research, Pune 411021, India.

However, to the best of our knowledge, there is no report on the temperature dependence of the phonons of the rare-earth stannate $\text{Pr}_2\text{Sn}_2\text{O}_7$, a dynamic spin-ice compound. In this paper, we report a detailed temperature-dependent Raman study of $\text{Pr}_2\text{Sn}_2\text{O}_7$ and compare it with its non-cubic (monoclinic) counterpart $\text{Pr}_2\text{Ti}_2\text{O}_7$. Apart from the Raman phonons, we identify two bands associated with electronic Raman scattering involving crystal field (CF) split J-multiplets of Pr^{3+} ($J = 4$) in $\text{Pr}_2\text{Sn}_2\text{O}_7$ near 135 and 460 cm^{-1} . A coupling between the 135 cm^{-1} CF mode and a low frequency ($\sim 150 \text{ cm}^{-1}$) phonon is observed indicating an important role of the crystal field interactions in this compound. Like in other pyrochlores, temperature dependence of some of the phonons in $\text{Pr}_2\text{Sn}_2\text{O}_7$ is anomalous, which is notably absent in the monoclinic titanate— $\text{Pr}_2\text{Ti}_2\text{O}_7$, thus indicating that the vacant sites in the cubic pyrochlore compounds play a crucial role in the strong phonon anharmonicities.

2. Experimental details

High purity Pr_6O_{11} (99.99 %) and TiO_2 (99.99 %) of stoichiometric amounts were mixed thoroughly and heated at 1200 °C for about 15 h which was then ground and isostatically pressed into rods of about 10 cm long and 5 mm diameter. These rods were sintered at 1400 °C in air for about 72 h and the procedure was repeated for several times until the compound $\text{Pr}_2\text{Ti}_2\text{O}_7$ was formed. Powder X-ray diffraction analysis of the samples confirmed the formation of monoclinic phase. Single crystals were then grown by using the floating-zone method by subjecting these rods in an infrared image furnace under flowing oxygen. Energy dispersive X-ray analysis on a scanning electron microscope and powder X-ray diffraction were further carried out on the powder obtained by crushing part of a single crystal sample which reconfirmed the pure $\text{Pr}_2\text{Ti}_2\text{O}_7$ phase. Moreover, neutron scattering study on this sample did not reveal any impurity phase [28]. The crystals were oriented along the principal crystallographic directions using the Laue back-reflection technique. On the other hand, we could obtain only polycrystals of $\text{Pr}_2\text{Sn}_2\text{O}_7$ by solid state sintering of respective high purity oxides. $\text{Pr}_2\text{Sn}_2\text{O}_7$ was pelletized for further studies. The phase purity of the sample was verified by powder X-ray diffraction analysis and the sample had a pyrochlore structure.

Raman spectroscopic measurements on cubic pyrochlore $\text{Pr}_2\text{Sn}_2\text{O}_7$ and monoclinic $\text{Pr}_2\text{Ti}_2\text{O}_7$ were performed from 12 K to room temperature in back-scattering geometry using the 514.5 nm line of an Ar^+ ion laser (Coherent Innova 300) with $\sim 15 \text{ mW}$ of power falling on the sample. Experimental details of the cryostat and the Raman instrument (spectral resolution $\sim 6 \text{ cm}^{-1}$) are given in our earlier work [16].

3. Results and discussion

3.1. Raman spectra of cubic (pyrochlore) $\text{Pr}_2\text{Sn}_2\text{O}_7$ and monoclinic $\text{Pr}_2\text{Ti}_2\text{O}_7$

Pyrochlores belong to the space group $Fd\bar{3}m(O_h^h)$ with a stoichiometry of $A_2B_2O_6O'$, where A^{3+} ions occupy the 16d Wyckoff sites and B^{4+} ions reside at the 16c sites, whereas the O and O' atoms are located at the 48f and 8b Wyckoff sites, respectively. Group theoretical analysis for this family of compounds predicts six-Raman active modes ($A_{1g} + E_g + 4F_{2g}$) and seven-infrared active modes ($7F_{1u}$). Fig. 1 shows Raman spectrum of $\text{Pr}_2\text{Sn}_2\text{O}_7$ at 12 K in the spectral range of 20–1050 cm^{-1} which has been fitted with 16 Lorentzians, labeled as M1 to M16 (see Table 1). Following previous Raman reports on this compound

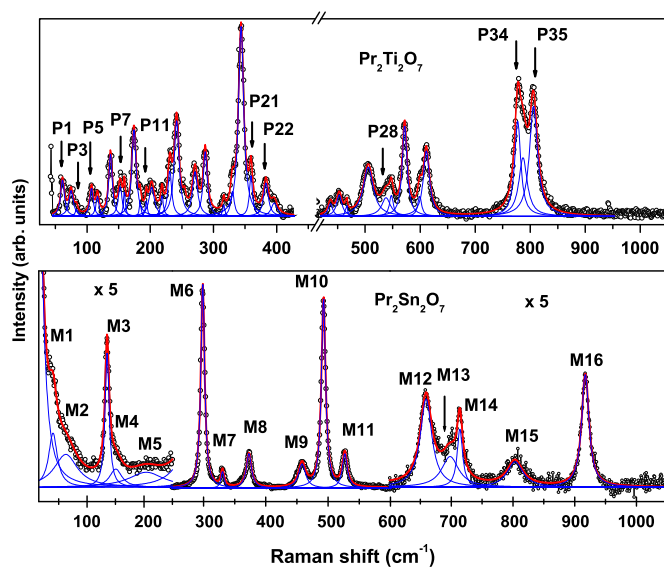


Fig. 1. (Color online) Raman spectra of $\text{Pr}_2\text{Sn}_2\text{O}_7$ and $\text{Pr}_2\text{Ti}_2\text{O}_7$ at 12 K. The intensity (of $\text{Pr}_2\text{Sn}_2\text{O}_7$ modes) has been rescaled in the region 20–250 cm^{-1} and 600–1050 cm^{-1} for a better view. The modes, labeled as M1 to M16, have been assigned as listed in Table 1. The Raman modes of $\text{Pr}_2\text{Ti}_2\text{O}_7$ are marked with arrows while the additional modes are due to photoluminescence transitions as discussed in the text.

Table 1

Experimental values of the mode frequencies of $\text{Pr}_2\text{Sn}_2\text{O}_7$.

Normal modes	At 12 K (cm^{-1})
M1 (Ph)	40
M2 (Ph)	63
M3 (CF)	135
M4 (Ph)	150
M5 (Ph)	204
M6 (Ph, F_{2g} , O–Sn–O bending, Sn–O and Pr–O stretching)	299
M7 (Ph, E_g , O–Sn–O bending, Sn–O and Pr–O stretching)	331
M8 (Ph, F_{2g})	373
M9 (CF)	458
M10 (Ph, A_{1g} , O–Sn–O bending and Sn–O stretching)	493
M11 (Ph, F_{2g} , O–Sn–O bending)	527
M12 (Ph, F_{2g} , Sn–O stretching)	659
M13 (Ph)	698
M14 (Ph)	714
M15 (Ph)	803
M16 (Ph)	917

Ph=Phonon, CF=crystal field transition.

[29–31], the modes can be assigned as follows: M6 as F_{2g} , M7 as E_g , M8 as F_{2g} , M10 as A_{1g} , M11 as F_{2g} and M12 as F_{2g} phonon. The low frequency modes M1, M2, M4 and M5 may arise due to disorder induced Raman activity of infrared active or silent phonons [31] and the high frequency modes M13 to M16 due to two-phonon Raman scattering, as also observed in other pyrochlore titanates [16,17,25,26]. The modes M3 and M9 are assigned to electronic Raman scattering involving crystal field transitions of Pr^{3+} [15,32] as discussed later.

The compound $A_2B_2O_7$ crystallizes with a pyrochlore structure [33] if the ratio of cationic radii, $\xi = r_{A^{3+}}/r_{B^{4+}}$, lies within the pyrochlore stability field, $1.46 < \xi < 1.80$. When ‘ ξ ’ is close to or smaller than 1.46, the defect fluorite structure is favored. However, when ξ is close to or greater than 1.80, monoclinic phase is favored. Not surprisingly, therefore, $\text{Pr}_2\text{Ti}_2\text{O}_7$ ($\xi \approx 1.86$) crystallizes with a monoclinic structure with P_21 space group [34]. Factor group analysis for this structure predicts six Raman modes ($3A+3B$) and six infrared modes ($3A+3B$). Fig. 1 shows the

Raman spectrum of $\text{Pr}_2\text{Ti}_2\text{O}_7$ at 12 K which can be fitted with 35 Lorentzians, labeled as P1 to P35. In order to distinguish between the Raman modes and photoluminescence lines of Pr^{3+} , we recorded the spectrum (not shown in Figure) at 300 K using a different laser excitation of 488 nm. This exercise suggests that the modes at $\sim 57 \text{ cm}^{-1}$ (P1), 86 cm^{-1} (P3), 115 cm^{-1} (P5), 149 cm^{-1} (P7), 194 cm^{-1} (P11), 354 cm^{-1} (P21), 385 cm^{-1} (P22), 525 cm^{-1} (P28), 782 cm^{-1} (P34) and 802 cm^{-1} (P35) are Raman modes. In a previous report [35], some of these modes were tentatively assigned as the Pr–O vibrations. The remaining modes of $\text{Pr}_2\text{Ti}_2\text{O}_7$ are attributed to the photoluminescence bands of Pr^{3+} [36,37] having different emission strengths at different laser excitation energies. The frequencies of the modes at 460 cm^{-1} (P26), 607 cm^{-1} (P32) and 802 cm^{-1} (P35) match well with those of the E_g , A_{1g} and F_{2g} mode frequencies of TiO_2 , as also pointed out in Ref. [35]. However, the modes P26 and P32 are not observed in the spectrum recorded using 488 nm laser excitation. Since the sample of $\text{Pr}_2\text{Ti}_2\text{O}_7$ is in single phase, as confirmed by the various techniques mentioned earlier, we, therefore, attribute the modes P26 and P32 as photoluminescence lines and P35 as a Raman mode.

3.2. Evolution of Raman spectra with temperature

3.2.1. $\text{Pr}_2\text{Sn}_2\text{O}_7$

Fig. 2 shows the evolution of Raman spectrum of $\text{Pr}_2\text{Sn}_2\text{O}_7$ at a few typical temperatures. The intensities of the modes M3 and M9 show a significant decrease with increasing temperature as shown in Fig. 3. Fig. 3 (top panels) also shows the ratio of integrated intensities of M3 and M9 modes with respect to that of mode M10 as a function of temperature. We have taken Mode M10 as a reference as it is intense and well resolved. Similar conclusions are drawn if M6 is taken as a reference. For comparison, we also show the relative intensity of the strongest

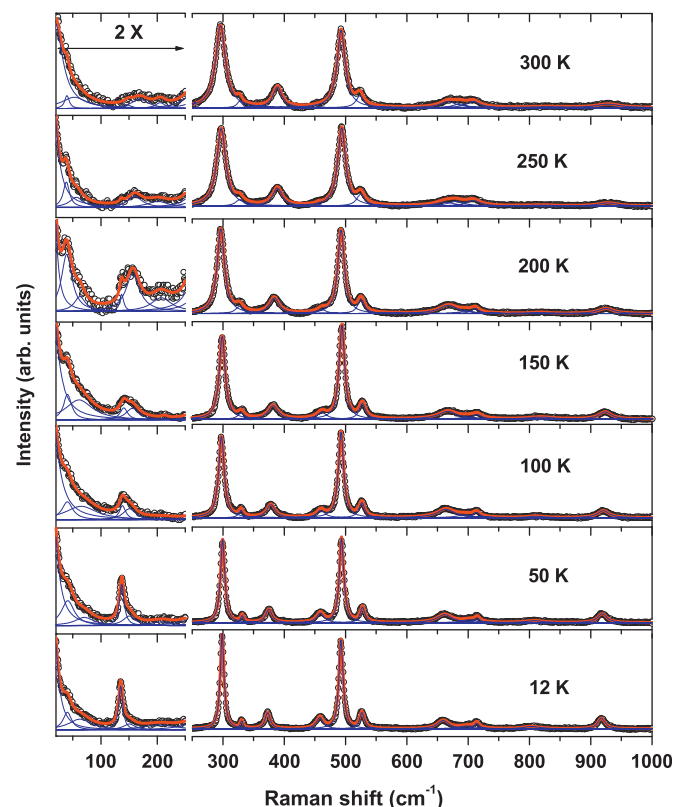


Fig. 2. (Color online) Raman spectra of $\text{Pr}_2\text{Sn}_2\text{O}_7$ at a few temperatures.

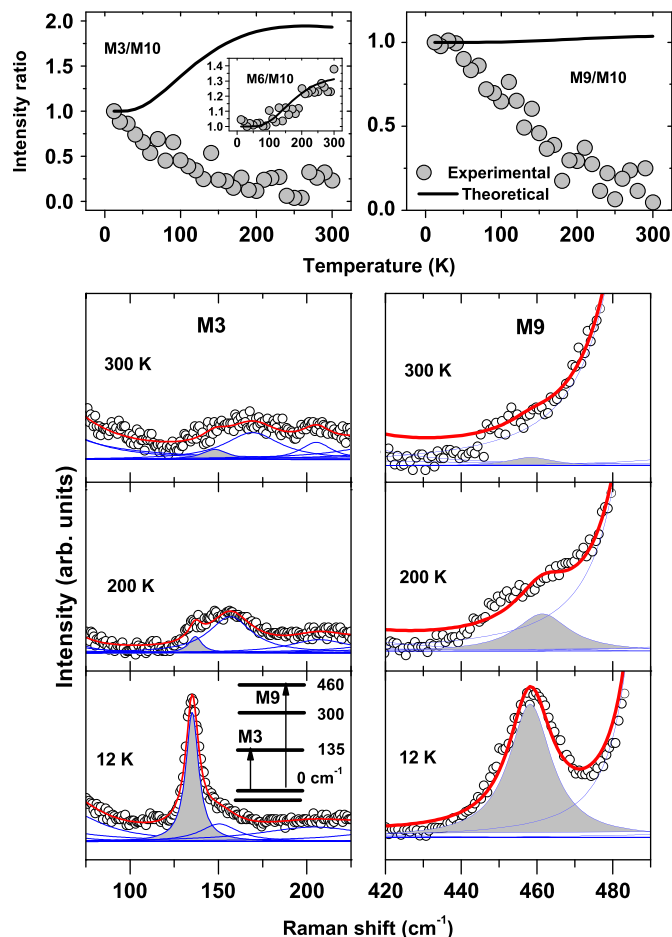


Fig. 3. (Color online) Evolution of the crystal field transition modes M3 and M9 of $\text{Pr}_2\text{Sn}_2\text{O}_7$ with temperature. The top panels show the integrated intensity ratio of the modes M3 and M9 with respect to the mode M10 of $\text{Pr}_2\text{Sn}_2\text{O}_7$. The intensity ratio of M6 to M10 is shown in the top inset. Inset of the left bottom panel shows the CF level scheme of Pr^{3+} in $\text{Pr}_2\text{Sn}_2\text{O}_7$ [15].

mode M6 with respect to the mode M10 (inset of top panel) which increases with temperature as expected due to the Stokes phonon population factor. This is also true for other phonon modes (therefore, not shown). The solid line (in the inset of the left top panel) is $(n(\omega_{M6}) + 1/n(\omega_{M10}) + 1)$, which fits the data as expected for a first order Raman mode. However, the modes M3 and M9 show a completely opposite trend from the expected population factor ratio, thus indicating a crystal field origin for these two Raman modes. In a crystalline electric field due to the surrounding oxygen ions with a D_{3d} symmetry, the nine-fold degenerate ground state (3H_4) of Pr^{3+} -ion splits into three doublets and three singlets. Recently, it has been shown that the ground state of these split levels has Ising-like anisotropy along the $\langle 111 \rangle$ direction [38]. Zhou et al. show that the first two excited singlets of Pr^{3+} in $\text{Pr}_2\text{Sn}_2\text{O}_7$ are at $E_1 = 19 \text{ meV}$ and $E_2 = 38 \text{ meV}$ [15], but they do not report the next higher excited levels. Based on this report we, suggest the modes M3 ($\sim 135 \text{ cm}^{-1} \equiv 17 \text{ meV}$) and M9 ($\sim 460 \text{ cm}^{-1} \equiv 57.5 \text{ meV}$) as the CF transitions from the ground state (E_0) to the first (E_1) and third (E_3) excited states of 3H_4 -manifold of Pr^{3+} -ion. The CF scheme is shown in the inset of the left bottom panel of 3. The CF transition from the ground state (E_0) to the second excited state (E_2) should be near 300 cm^{-1} ($\sim 38 \text{ meV}$) which can overlap with the intense F_{2g} (M6) Raman phonon.

In Fig. 4, we present the temperature dependence of frequencies of the modes M3, M4, M6 to M10, M12, and M14 to M16.

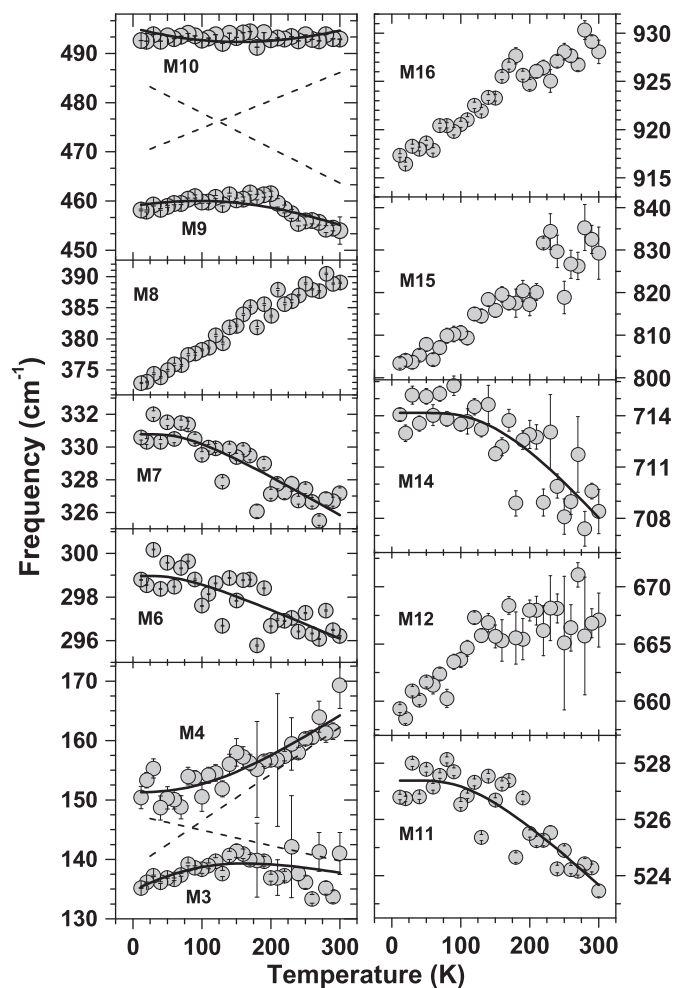


Fig. 4. Temperature dependence of frequency of the modes M3, M4, M6, M7, M8, M9, M10, M11, M12, M14, M15 and M16 of $\text{Pr}_2\text{Sn}_2\text{O}_7$. Crystal field mode M3 and phonon M4 are fitted with equations for coupled excitations revealing a coupling between them. Dashed lines are the anticipated temperature dependence of the M3 and M4 modes when they are uncoupled. Modes M9 and M10 also show a similar coupling. Modes M6, M7, M11 and M14 show normal temperature dependence and are fitted by cubic anharmonic equation for phonons [41]. The modes M8, M12, M15 and M16 show anomalous temperature dependence.

It can be seen that the temperature dependence of the frequencies of modes M3 (CF) and M4 (phonon) are unusual and signal a coupling between these two excitations. Taking two coupled oscillator model with a coupling strength V between the modes, the renormalized frequencies of the modes M3 and M4 will be [39]:

$$\omega_{\pm} = \frac{1}{2}[(\omega_3 + \omega_4) \pm \sqrt{(\omega_3 + \omega_4)^2 - 4(\omega_3\omega_4 - V^2)}] \quad (1)$$

where ω_3 and ω_4 are the uncoupled mode frequencies. With an assumption that the uncoupled mode frequencies (ω_3 and ω_4) are linear in temperature, $\omega_3 = \omega_3(0) + a_3T$ and $\omega_4 = \omega_4(0) + a_4T$ (as shown by the dashed lines in Fig. 4), we fit $\omega^+(T)$ (M4) and $\omega^-(T)$ (M3) to the data (fit shown by solid lines). The parameters obtained from the good fit are $\omega_3(0) = 139 \text{ cm}^{-1}$, $a_3 = 0.08 \text{ cm}^{-1}/\text{K}$, $\omega_4(0) = 148 \text{ cm}^{-1}$, $a_4 = -0.03 \text{ cm}^{-1}/\text{K}$, and $V = 7 \text{ cm}^{-1}$. We also find that the distance of closest approach ($\sim 13 \text{ cm}^{-1}$) between the two modes is nearly double the coupling strength, as expected for coupled excitations [40]. As seen in Fig. 4, the A_{1g} phonon (M10) remains nearly constant with temperature which is different from other pyrochlore titanates where it shows an anomalous softening (by $\sim 7 \text{ cm}^{-1}$) upon cooling from room temperature to 10 K [16–20]. This indicates a possible coupling between the two modes

M9 (CF) and M10 (phonon). Using Eq. (1) and identifying ω^+ with M10 and ω_- with the M9 mode, we find the parameters for modes M9 and M10 as: $\omega_9(0) = 469 \text{ cm}^{-1}$, $a_9 = 0.06 \text{ cm}^{-1}/\text{K}$, $\omega_{10}(0) = 485 \text{ cm}^{-1}$, $a_{10} = -0.07 \text{ cm}^{-1}/\text{K}$, and $V = 16 \text{ cm}^{-1}$. The fits are shown by solid lines. Here also, the dashed lines show the temperature dependence of the corresponding uncoupled mode frequencies.

As shown in Fig. 4, the modes M6, M7, M11 and M14 show a normal temperature dependence, i.e., frequency increases with decreasing temperature. However, the modes M8, M12, M15, and M16 show an anomalous temperature dependence. A similar temperature-dependent anomaly is also observed in the phonons of other pyrochlore titanates [16–20] and attributed to phonon-phonon anharmonic interactions.

3.2.2. $\text{Pr}_2\text{Ti}_2\text{O}_7$

In Fig. 5, we present the temperature dependence of the phonon modes of $\text{Pr}_2\text{Ti}_2\text{O}_7$. Interestingly, no phonon anomaly is seen in this compound. The absence of phonon anomalies in $\text{Pr}_2\text{Ti}_2\text{O}_7$, may be understood in the following way: in pyrochlore structure the Pr occupies the 16d sites, Sn are at 16c while the O and O' are at 48f and 8b sites thus leaving the 8a-sites vacant. The Pr atoms form a tetrahedral network with the O_{8b} atoms at the center of each tetrahedron, while Sn atoms form another network of tetrahedra with the 8a-vacant sites at the center of each of the Sn-tetrahedron. Due to this vacancy, the Sn atoms will have larger vibrational amplitudes thus making the phonons highly anharmonic. The absence of vacant sites in monoclinic structure,

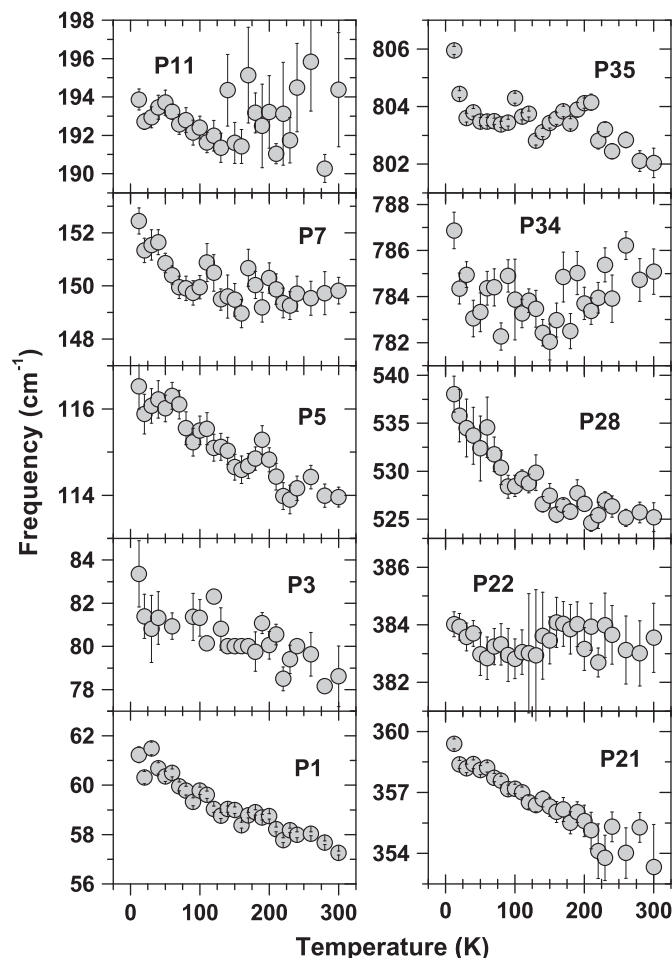


Fig. 5. Temperature dependence of frequency of Raman modes of $\text{Pr}_2\text{Ti}_2\text{O}_7$.

therefore, reduces this large anharmonicity, resulting into a normal temperature dependence of the phonons.

4. Summary and conclusion

Raman spectra of the pyrochlore “dynamic spin-ice” compound $\text{Pr}_2\text{Sn}_2\text{O}_7$ at different temperatures ranging from 12 to 300 K are compared with those of its non-cubic (monoclinic) counterpart $\text{Pr}_2\text{Ti}_2\text{O}_7$. In $\text{Pr}_2\text{Sn}_2\text{O}_7$, we observe two crystal field (CF) transitions are observed at $\sim 135 \text{ cm}^{-1}$ (M3) and 460 cm^{-1} (M9), along with various Raman phonons. With the D_{3d} point symmetry of Pr^{3+} -ions surrounded by six-planar O^{2-} -ions and two-apical O'^{2-} -ions in pyrochlore, the degenerate ground state of $^3\text{H}_4$ -manifold splits into 3-doublets and 3-singlets, of which the ground state is a doublet and the first three excited states are singlets [15,32]. We attribute the $\sim 135 \text{ cm}^{-1}$ mode as the transition from the ground state to the first excited singlet and the $\sim 460 \text{ cm}^{-1}$ mode as the transition to the third excited singlet. The intensities of these two CF modes decrease significantly with increasing temperature, making them too weak to be seen at room temperature, thus suggesting their origin as CF transitions. We find that the CF mode at $\sim 135 \text{ cm}^{-1}$ (M3) couples with the phonon M4 at $\sim 150 \text{ cm}^{-1}$. The two-mode coupled model fitted to the temperature dependence of the M3 and M4 modes gives a measure of the CF-phonon coupling to be $\sim 1 \text{ meV}$. Similarly, the CF mode M9 couples with the A_{1g} phonon M10 with a coupling strength of $\sim 2 \text{ meV}$.

The temperature dependence of various modes of $\text{Pr}_2\text{Sn}_2\text{O}_7$ are investigated. The phonons near $\sim 300 \text{ cm}^{-1}$ (M6), $\sim 330 \text{ cm}^{-1}$ (M7), $\sim 525 \text{ cm}^{-1}$ (M11) and 710 cm^{-1} (M14) show a normal temperature dependence. However, the phonons M8 $\sim 380 \text{ cm}^{-1}$, M12 $\sim 665 \text{ cm}^{-1}$, M15 $\sim 830 \text{ cm}^{-1}$ and M16 $\sim 920 \text{ cm}^{-1}$ show anomalous softening with decreasing temperature. This anomalous behavior is very similar to the phonon anomalies observed in other pyrochlore titanates [16–20]. Since no long range magnetic order exists in $\text{Pr}_2\text{Sn}_2\text{O}_7$ above 200 mK [15], we attribute these phonon anomalies to phonon–phonon anharmonic interactions that arise due to the unusually large vibrational amplitudes of the B-type atoms (Sn^{4+}) that form a tetrahedron centered around the $8a$ -vacant sites. In contrast, no phonon anomaly is seen in monoclinic $\text{Pr}_2\text{Ti}_2\text{O}_7$.

We, therefore, conclude that the strong phonon–phonon anharmonicity is an inherent property of the pyrochlore ($A_2B_2O_7$) structure with an appropriate range of cationic radii ratio ($\zeta = r_A^{3+}/r_B^{4+}$) such that it retains the (unusually) large vibrational amplitudes of the B-type atoms. The effect of replacement of smaller B^{4+} -ions by heavier and bigger ions on the phonon anharmonicities will be interesting to explore.

Acknowledgments

We thank the Indo-French Centre for Promotion of Advanced Research (IFCPAR), Centre Franco-Indien pour la Promotion de la Recherche Avancée (CEFIPRA) for financial support under Project no. 3108-1. AKS thanks the Department of Science and Technology (DST), India, for partial financial support.

References

- [1] A.P. Ramirez, *Annu. Rev. Mater. Sci.* 24 (1994) 453–480.
- [2] R. Moessner, A.P. Ramirez, *Phys. Today* 59 (2) (2006) 24–29.
- [3] J.E. Greedan, *J. Alloys Compd.* 408–412 (2006) 444–455.

- [4] J.S. Gardner, B.D. Gaulin, A.J. Berlinsky, P. Waldron, S.R. Dunsiger, N.P. Raju, J.E. Greedan, *Phys. Rev. B* 64 (2001) 224416.
- [5] S.-W. Han, J.S. Gardner, C.H. Booth, *Phys. Rev. B* 69 (2004) 024416.
- [6] K.C. Rule, J.P.C. Ruff, B.D. Gaulin, S.R. Dunsiger, J.S. Gardner, J.P. Clancy, M.J. Lewis, H.A. Dabkowska, I. Mirebeau, P. Manuel, Y. Qiu, J.R.D. Copley, *Phys. Rev. Lett.* 96 (2006) 177201.
- [7] M.J. Harris, S.T. Bramwell, D.F. McMorrow, T. Zeiske, K.W. Godfrey, *Phys. Rev. Lett.* 79 (1997) 2554–2557.
- [8] S.T. Bramwell, M.J. Harris, B.C. den Hertog, M.J.P. Gingras, J.S. Gardner, D.F. McMorrow, A.R. Wildes, A.L. Cornelius, J.D.M. Champion, R.G. Melko, T. Fennell, *Phys. Rev. Lett.* 87 (2001) 047205.
- [9] T. Fennell, O.A. Petrenko, B. Fåk, S.T. Bramwell, M. Enjalran, T. Yavorskii, M.J.P. Gingras, R.G. Melko, G. Balakrishnan, *Phys. Rev. B* 70 (2004) 134408.
- [10] G.C. Lau, R.S. Freitas, B.G. Ueland, B.D. Muegge, E.L. Duncan, P. Schiffer, R.J. Cava, *Nat. Phys.* 2 (2006) 249–253.
- [11] A.P. Ramirez, A. Hayashi, R.J. Cava, R. Siddharthan, B.S. Shastry, *Nature* 399 (1999) 333–335.
- [12] L. Pauling, *The Nature of Chemical Bond*, Cornell University Press, Ithaca, NY, 1945, pp. 301–304.
- [13] K. Matsuhira, Y. Hinatsu, K. Tenya, T. Sakakibara, *J. Phys.: Condens. Matter* 12 (2000) L649–L656.
- [14] I. Mirebeau, A. Apetrei, J. Rodríguez-Carvajal, P. Bonville, A. Forget, D. Colson, V. Glazkov, J.P. Sanchez, O. Isnard, E. Suard, *Phys. Rev. Lett.* 94 (2005) 246402.
- [15] H.D. Zhou, C.R. Wiebe, J.A. Janik, L. Balicas, Y.J. Yo, Y. Qiu, J.R.D. Copley, J.S. Gardner, *Phys. Rev. Lett.* 101 (2008) 227204.
- [16] S. Saha, S. Singh, B. Dkhil, S. Dhar, R. Suryanarayanan, G. Dhailenne, A. Revcolevschi, A.K. Sood, *Phys. Rev. B* 78 (2008) 214102.
- [17] M. Mączka, M.L. Sanjuan, A.F. Fuentes, K. Hermanowicz, J. Hanuza, *Phys. Rev. B* 78 (2008) 134420.
- [18] M. Mączka, J. Hanuza, K. Hermanowicz, A.F. Fuentes, K. Matsuhira, Z. Hiroi, *J. Raman Spectrosc.* 39 (2008) 537–544.
- [19] T.T.A. Lummen, I.P. Handayani, M.C. Donker, D. Fausti, G. Dhailenne, P. Berthet, A. Revcolevschi, P.H.M. van Loosdrecht, *Phys. Rev. B* 77 (2008) 214310.
- [20] C.Z. Bi, J.Y. Ma, B.R. Zhao, Z. Tang, D. Yin, C.Z. Li, D.Z. Yao, J. Shi, X.G. Qiu, *J. Phys.: Condens. Matter* 17 (2005) 5225–5233.
- [21] F.X. Zhang, B. Manoun, S.K. Saxena, C.S. Zha, *Appl. Phys. Lett.* 86 (2005) 181906.
- [22] F.X. Zhang, S.K. Saxena, *Chem. Phys. Lett.* 413 (2005) 248–251.
- [23] S. Saha, D.V.S. Muthu, C. Pascanut, N. Drago, R. Suryanarayanan, G. Dhailenne, A. Revcolevschi, S. Karmakar, S.M. Sharma, A.K. Sood, *Phys. Rev. B* 74 (2006) 064109.
- [24] S. Singh, S. Saha, S.K. Dhar, R. Suryanarayanan, A.K. Sood, A. Revcolevschi, *Phys. Rev. B* 77 (2008) 054408.
- [25] S. Saha, D.V.S. Muthu, S. Singh, B. Dkhil, R. Suryanarayanan, G. Dhailenne, H.K. Poswal, S. Karmakar, S.M. Sharma, A. Revcolevschi, A.K. Sood, *Phys. Rev. B* 79 (2009) 134112.
- [26] M. Mączka, M.L. Sanjuan, A.F. Fuentes, L. Macalik, J. Hanuza, K. Matsuhira, Z. Hiroi, *Phys. Rev. B* 79 (2009) 214437.
- [27] S. Saha, P. Ghalsasi, D. V. S. Muthu, S. Singh, R. Suryanarayanan, G. Dhailenne, A. Revcolevschi, A. K. Sood, Unpublished, 2010.
- [28] S. Singh, et al., private communication.
- [29] M.T. Vandendorpe, E. Husson, J.P. Chatry, D. Michel, *J. Raman Spectrosc.* 14 (1983) 63–71.
- [30] T.T. Zhang, K.W. Li, J. Zeng, Y.L. Wang, X.M. Song, H. Wang, *J. Phys. Chem. Solids* 69 (2008) 2845–2851.
- [31] H.C. Gupta, S. Brown, N. Rani, V.B. Gohel, *Int. J. Inorg. Mater.* 3 (2001) 983–986.
- [32] J. van Duijn, K.H. Kim, N. Hur, D. Adroja, M.A. Adams, Q.Z. Huang, M. Jaime S.-W. Cheong, C. Broholm, T.G. Perring, *Phys. Rev. Lett.* 94 (2005) 177201.
- [33] M.A. Subramanian, G. Aravamudan, G.V. Subba Rao, *Prog. Solid Stat. Chem.* 15 (1983) 55–143.
- [34] Z. Shao, S. Saitzek, P. Roussel, M. Huvé, R. Desfeux, O. Mentré, F. Abraham, *J. Cryst. Growth* 311 (2009) 4134–4141.
- [35] K. Krishnakutty, K.R. Dayas, *Bull. Mater. Sci.* 31 (2008) 907–918.
- [36] P.T. Djalio, P. Boutinaud, R. Mahiou, J.C. Cousseins, *J. Alloys and Compd.* 275–277 (1998) 307–310.
- [37] P.T. Djalio, P. Boutinaud, R. Mahiou, *J. Alloys and Compd.* 341 (2002) 139–143.
- [38] K. Matsuhira, Y. Hinatsu, K. Tenya, H. Amitsuka, T. Sakakibara, *J. Phys. Soc. Jpn.* 71 (2002) 1576–1582.
- [39] E.T. Heyen, R. Wegerer, E. Schönherr, M. Cardona, *Phys. Rev. B* 44 (1991) 10195.
- [40] J.F. Scott, *Phys. Rev. Lett.* 24 (1970) 1107.
- [41] M. Balkanski, R.F. Wallis, E. Haro, *Phys. Rev. B* 28 (1983) 1928.